

## Adsorptive removal of Fe(III) using gallic acid anchored iron magnetic nano-adsorbents synthesized via two different routes under microwave irradiation

Asmaa M Abdel Rahim\*, Salwa A Ahmed & Ezzat M Soliman  
Chemistry Department, Faculty of Science, Minia University, El-Minia 61511, Egypt  
Email: moheyeldin51@gmail.com

*Received 11 July 2018; revised and accepted 20 December 2019*

Under microwave solvent free conditions, bare iron magnetic nanoparticles ( $\text{Fe}_3\text{O}_4$ -MNPs) have been silica coated, amine functionalized and gallic acid grafted, in presence and absence of tetraethylorthosilicate (TEOS). The synthesized adsorbents in both cases have been followed up by Fourier transform infrared, scan electron microscopy and transmission electron microscopy analyses to verify and compare the progress of surface modification. The effects of various parameters on the adsorption efficiency of Fe(III) such as pH of solution, amount of adsorbent and contact time have been studied and optimized. The adsorbents  $\text{Fe}_3\text{O}_4$ -MNPs-SiO<sub>2</sub>-CPTMS-1,2-EDA-GA and MNPs-CPTMS-1,2-EDA-GA exhibit higher Fe(III) capacities (4.980 and 4.700 mmol/g) than their analogous  $\text{Fe}_3\text{O}_4$ -MNPs-SiO<sub>2</sub>-APTMS-GA and  $\text{Fe}_3\text{O}_4$ -MNPs-APTMS-GA (4.324 and 4.230 mmol/g). The studies of sorption kinetics showed rapid sorption dynamics by a second-order kinetic model, suggesting chemisorption mechanism. Fe(III) adsorption equilibrium data have been fitted well to the Langmuir isotherm. The results of medium stability as criteria for potential coating and values of metal uptake capacity support the possibility of the direct use of alkoxysilanes as an alternative to TEOS not only for coating but also for amine functionalization. This is strengthened by almost equal capability of gallic acid anchored adsorbents for extraction of trace concentrations of Fe(III) spiked natural water samples.

**Keywords:** Iron magnetic nanoparticles, Tetraethylorthosilicate, Gallic acid, Microwave irradiation, Transmission electron microscopy

Separation technique based on using magnetic nanoparticles (MNPs) received growing interest in the last few years<sup>1</sup>. It provides great potential for applications in drug delivery<sup>2</sup>, cell separation<sup>3</sup>, enzymes and proteins immobilization<sup>4</sup>. In addition, MNPs anchored selective functional groups have been extensively implemented for separation and preconcentration in trace metal analysis<sup>5</sup>, removal of organic and inorganic pollutants from water samples as well<sup>6-9</sup>. Among MNPs, iron oxides, especially magnetite ( $\text{Fe}_3\text{O}_4$ ) has received considerable attention due to the pronounced advantages related to their nano-size, high surface area, fast kinetics and great adsorption capacity for target analytes. This is accompanied by easy separation process under the influence of external magnetic field<sup>10</sup>. However, particles of  $\text{Fe}_3\text{O}_4$  in aqueous medium tend to form large aggregates resulting in reducing their magnetic properties. In addition, the lack of selectivity and medium effects minimize their use in complex matrices. To overcome the above limitations, protection process for the surfaces of  $\text{Fe}_3\text{O}_4$ -MNPs is essential. The protection which is usually achieved by

coating with inorganic components such as silica or alumina or organic molecules like polymers or surfactants lead to improved their chemical stability, preventing their oxidation and aggregation<sup>11-14</sup>. In this respect, tetraethylorthosilicate (TEOS) is the first and predominately used as inorganic protection agent for coating, rather than organic molecules<sup>15</sup>. In addition, the surface silanol (Si-OH) groups incorporated silica coated  $\text{Fe}_3\text{O}_4$ -MNPs enable special functional groups for binding with the desired adsorbate<sup>16</sup>. Recently, it was observed that, alkoxysilane linkers were utilized directly for coating and surface functionalization of MNPs<sup>17</sup>. These organic silanes are bi-functional molecules containing mainly trialkoxy group able for binding covalently to the free hydroxyl groups at the surface of the particles and a specific functional group (e.g.,  $-\text{NH}_2$ ,  $-\text{OH}$ ,  $-\text{SH}$ ,  $-\text{Cl}$ , etc.) that determines the chemical affinity of the surface. This surface can be further functionalized using organic complexing agents for employing as adsorbents in solid phase extraction (SPE) for trace analysis<sup>18</sup>. Among these organic complexing agents, gallic acid (3,4,5-trihydroxy benzoic acid) is a strong chelating agent.

It forms complexes of high stability with iron which is attached to gallic acid through two adjacent OH<sup>19</sup>.

The aim of this paper was directed toward surface modification of iron MNPs with silica coating via direct reaction with alkoxy silane, as alternative to the conventional mode adapting TEOS for the formation of new combined nanomagnetic sorbent. For this purpose Fe<sub>3</sub>O<sub>4</sub>-MNPs as adsorbed core was functionalized by amine group moiety in presence and absence of TEOS, followed by gallic acid grafting. The efficiency of the coating mode in both cases was compared and assessed by Cu(II) and Fe(III) uptake, stability studies and application for retaining trace concentrations of Fe(III) spiked natural water samples. Owing to the immense potential and the well-known benefits for utilization of microwave (MW) in synthetic chemistry<sup>20-22</sup>, all modifications steps performed on Fe<sub>3</sub>O<sub>4</sub>-MNPs were achieved using MW irradiation instead of conventional heating.

## Materials and Methods

### Experimental

Analytical reagent grade ferrous sulphate heptahydrate (FeSO<sub>4</sub>·7H<sub>2</sub>O), ferric chloride hexahydrate (FeCl<sub>3</sub>·6H<sub>2</sub>O) and copper chloride dihydrate (CuCl<sub>2</sub>·2H<sub>2</sub>O) were purchased from Aldrich Chemical Company, USA. Tetraethylorthosilicate (TEOS) was purchased from Sigma Alpha, India. Sodium hydroxide, hydrochloric acid, aminopropyltrimethoxysilane (APTMS), chloropropyltrimethoxysilane (CPTMS), 1,2-ethylenediamine (1,2-EDA), 1,3-dicyclohexylcarbodiimide (DCC) and gallic acid (GA) were purchased from BDH, UK.

### Apparatus

A Fisher Scientific Accumet pH-meter (Model 825, Germany) calibrated against two standard buffer solutions at pH 4.0 and 9.2 was used for pH measurements. Wrist Action mechanical shaker model 75 (manufactured by Burrell Corporation Pittsburgh, PA, USA) was used for shaking. Microwave oven (KOR-131G, Korea) emitting 2.450 GHz microwave frequency, 200–240 V, 50 Hz, microwave input power: 1350 W, microwave energy output: 1000 W, was used for silica coating and functionalization. Fourier transform infrared (FT-IR) analysis was measured by Perkin Elmer FT-IR system spectrometer (England) in the range 4000–400 cm<sup>-1</sup>. X-ray diffraction (XRD) analysis was carried out using a Philips Co. PW 1370 X-ray diffractometer with Ni filtered CuK radiation (1.5406 Å). Scanning

electron microscopy (SEM) analysis was obtained using JSM-5400 LV JEOL (Japan). Transmission electron microscopy (TEM) analysis was obtained using JSM-5400 LV JEOL (Japan).

### Synthesis of Fe<sub>3</sub>O<sub>4</sub>-nanoparticles (Fe<sub>3</sub>O<sub>4</sub>-MNPs)

Magnetic nanoparticles (Fe<sub>3</sub>O<sub>4</sub>-MNPs) were prepared by the co-precipitation method described before<sup>15</sup>.

### Coating of Fe<sub>3</sub>O<sub>4</sub>-MNPs in presence of TEOS followed by amine functionalization using microwave irradiation

2.0 mL of TEOS was added to 1.0 g of Fe<sub>3</sub>O<sub>4</sub>-MNPs and well mixed. The mixture was irradiated for 30 min at 200 W power (as appears in the oven scale refers to 20% of the value of the microwave output power). The resulted phase was then washed with hot water (60 °C) to remove the residues and excess of TEOS and left to dry in an oven at 60 °C to give silica coated magnetite (Fe<sub>3</sub>O<sub>4</sub>-MNPs-SiO<sub>2</sub>) as dark brown product<sup>23</sup>.

2.0 mL of aminopropyltrimethoxysilane (APTMS) was added to 1.0 g of Fe<sub>3</sub>O<sub>4</sub>-MNPs-SiO<sub>2</sub>. The mixture was irradiated for 20 min at a power of 200 W. The resulted phase was then washed and dried as previous to give dark brown product (Fe<sub>3</sub>O<sub>4</sub>-MNPs – SiO<sub>2</sub>– APTMS).

2.0 mL of chloropropyltrimethoxysilane (CPTMS) was added to 1.0 g of Fe<sub>3</sub>O<sub>4</sub>-MNPs-SiO<sub>2</sub>. The mixture was irradiated for 20 min at a power of 200 W. The resulted phase was then washed and dried to give dark brown product (Fe<sub>3</sub>O<sub>4</sub>-MNPs – SiO<sub>2</sub>– CPTMS). 2.0 mL of 1,2-ethylenediamine (1,2-EDA) was added to 1.0 g of Fe<sub>3</sub>O<sub>4</sub>-MNPs-SiO<sub>2</sub>-CPTMS. The mixture was irradiated in power 200 W for 10 min. The resulted phase was then washed and dried to give brown product (Fe<sub>3</sub>O<sub>4</sub>-MNPs-SiO<sub>2</sub>-CPTMS-1,2-EDA).

### Direct coating and amine functionalization (in absence of TEOS) of Fe<sub>3</sub>O<sub>4</sub>-MNPs using alkoxy silanes (APTMS and CPTMS) under microwave irradiation

2.0 mL of APTMS was added to 1.0 g of Fe<sub>3</sub>O<sub>4</sub>-MNPs. The mixture was irradiated at 200 W power for 20 min. The resulting phase was then washed with hot water (60 °C) to remove the residues and excess silylating agent and left to dry in an oven at 60 °C to give dark brown product (Fe<sub>3</sub>O<sub>4</sub>-MNPs-APTMS).

2.0 mL of CPTMS was added to 1.0 g of Fe<sub>3</sub>O<sub>4</sub>-MNPs. The mixture was irradiated at 200 W power for 20 min. The resulting phase was then washed with hot water (60 °C) to remove the residues and excess silylating agent and left to dry in an oven at 60 °C to

give dark brown product ( $\text{Fe}_3\text{O}_4\text{-MNPs-CPTMS}$ ). 2.0 mL of 1,2-EDA was added to 1.0 g of  $\text{Fe}_3\text{O}_4\text{-MNPs-CPTMS}$ . The mixture was irradiated at 200 W power for 10 min. The resulted phase was then washed and dried to give brown product ( $\text{Fe}_3\text{O}_4\text{-MNPs-CPTMS-1,2-EDA}$ ).

#### Amine functionalized magnetic nano-adsorbents as precursors for anchoring gallic acid via microwave technique

1.0 g of each  $\text{Fe}_3\text{O}_4\text{-MNPs-SiO}_2\text{-APTMS}$ ,  $\text{Fe}_3\text{O}_4\text{-MNPs-SiO}_2\text{-CPTMS-1,2-EDA}$  and  $\text{Fe}_3\text{O}_4\text{-MNPs-APTMS}$  and  $\text{Fe}_3\text{O}_4\text{-MNPs-CPTMS-1,2-EDA}$  in presence of 2.0 g of DCC used for peptide synthesis<sup>24</sup> was well mixed and subjected to a microwave irradiation power of 200 W for 5 min. The product (dark brown color) mixed with 10.0 g gallic acid (white color), well grinded and further irradiated

at 200 W power for 5 min. The resulted adsorbent was then washed with hot water (60 °C) to remove the residues and excess of gallic acid and left to dry in an oven at 60 °C to give dark yellow products, Fig. 1. The irradiation time by microwave was determined based on obtaining homogeneous product (solid state product with a uni-color and shape). A suggested representation for silica coating of  $\text{Fe}_3\text{O}_4$  using TEOS or alkoxysilanes, amine functionalization and gallic acid grafting under microwave solvent-free conditions is given in Scheme 1.

#### Batch adsorption experiments

##### Effect of contact time

In adsorption experiments 50.0 mg of each adsorbent was mixed with 0.5 mL of 0.1 mol L<sup>-1</sup> of

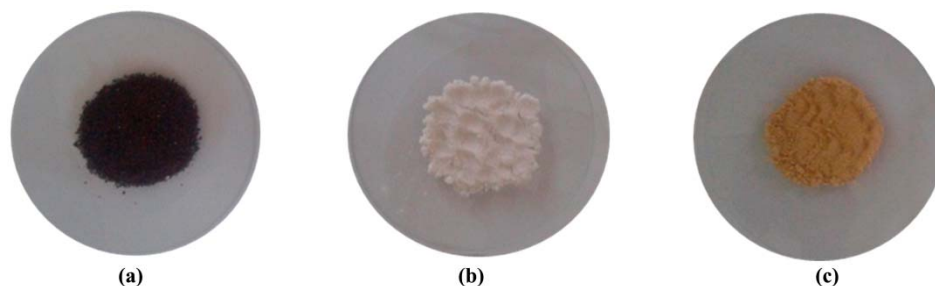
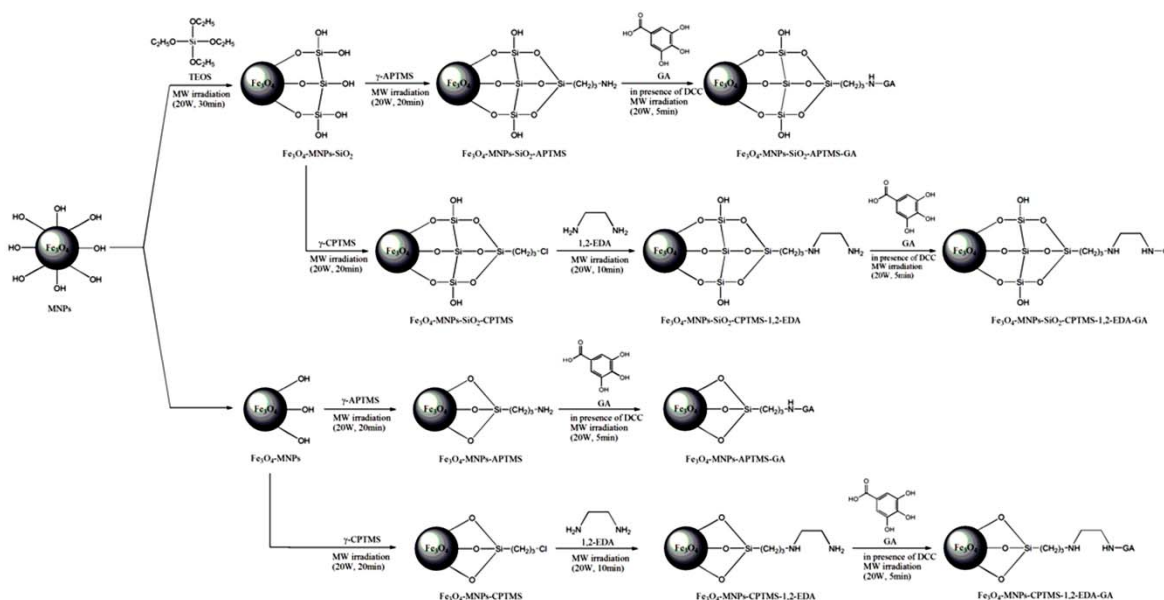


Fig. 1 — Colors of amine functionalized magnetic nano-adsorbents before and after anchoring gallic acid (GA) (a)  $\text{Fe}_3\text{O}_4\text{-MNPs-SiO}_2\text{-APTMS}$  or  $\text{Fe}_3\text{O}_4\text{-MNPs-SiO}_2\text{-CPTMS-1,2-EDA}$  or  $\text{Fe}_3\text{O}_4\text{-MNPs-APTMS}$  or  $\text{Fe}_3\text{O}_4\text{-MNPs-CPTMS-1,2-EDA}$ , (b) gallic acid and (c)  $\text{Fe}_3\text{O}_4\text{-MNPs-SiO}_2\text{-APTMS-GA}$  or  $\text{Fe}_3\text{O}_4\text{-MNPs-SiO}_2\text{-CPTMS-1,2-EDA-GA}$  or  $\text{Fe}_3\text{O}_4\text{-MNPs-APTMS-GA}$  or  $\text{Fe}_3\text{O}_4\text{-MNPs-CPTMS-1,2-EDA-GA}$ .



A suggested Scheme for gallic acid (GA) anchored iron magnetic nano-adsorbents synthesized utilizing alkoxysilanes in presence and absence of tetraethylorthosilicate via microwave irradiation

Scheme 1

Fe(III) in 100 mL measuring flask. The pH adjustment by using 1.0 M HCl and 0.1 M NaOH at pH range 2.0–4.0. Then the total volume was completed to 50.0 mL by DDW and was shaken at selected time (5.0, 15.0, 30.0, 45.0 and 60.0 s). The combined nano-sorbent with Fe(III) was magnetically separated from solution under the effect of an external magnetic field and the free metal ion solution was transferred to a conical flask. The metal concentration in the aqueous solutions was determined by complexometric EDTA titration. The adsorption capacity  $q$  (mmol/g) were obtained as follows:  $q = [(C_o - C_f)V/m]$ ; where  $C_o$  and  $C_f$  are the initial and final concentrations ( $\text{mol L}^{-1}$ ) of metal ion in the aqueous solution, respectively,  $V$  the volume of metal ion solution and  $m$  is the weight of adsorbent (g).

#### Effect of adsorbent dosage

The effect of nano-adsorbent dosage on the metal uptake of Fe(III) was studied by the batch equilibrium technique and various masses (from 10.0 to 100.0 mg-sorbent). The optimum conditions were used, pH 4.0 and contact time 5.0 s. The procedure was completed as described above.

#### Stability of the amine functionalized magnetic nano-adsorbents as a function of the pH of the medium

The stability of the magnetic nano-adsorbents (in presence and absence of TEOS) was investigated in pH range 1.0–10.0 using HCl and NaOH under

static conditions<sup>25</sup>. In this study, 100.0 mg of the adsorbent was soaked in 25.0 mL of the selected pH solution in 50 mL measuring flask for 60 min, then mechanically shaken for another 60 min. The solution was decanted, and then the adsorbent washed with doubly distilled water (DDW), magnetically separated and dried. To explore the effect of medium on stability, 50.0 mg of the treated adsorbent along with untreated one were used to evaluate Cu(II) adsorption capacity at optimum batch conditions (pH= 7.0 and shaking time<sup>26</sup> = 5 s). The obtained values of Cu(II) uptake were compared with that of the standard untreated one.

## Results and Discussion

#### X-ray diffraction of Fe<sub>3</sub>O<sub>4</sub>-MNPs

To affirm the Fe<sub>3</sub>O<sub>4</sub> structure, X-ray diffraction patterns (XRD) were employed. The powder XRD pattern of the synthesized magnetic nanoparticles was close to the pattern for crystalline magnetite<sup>27</sup> Fe<sub>3</sub>O<sub>4</sub> as shown in Fig. 2. Using the most intense peak in Fe<sub>3</sub>O<sub>4</sub> nanoparticles XRD pattern, the particle sizes of approximately 9.8–18.8 nm was estimated by the Debye–Scherer formula<sup>28</sup>. These values were consistent with the results obtained before from the TEM image of Fe<sub>3</sub>O<sub>4</sub>-MNPs<sup>23</sup>. The characteristic peaks of pure Fe<sub>3</sub>O<sub>4</sub>-MNPs nanoparticles at  $2\theta/\text{deg.} = 30.1, 35.4, 43.9, 53.4, 57.0$  and  $62.6$  confirming the presence of the crystalline structure of the magnetite.

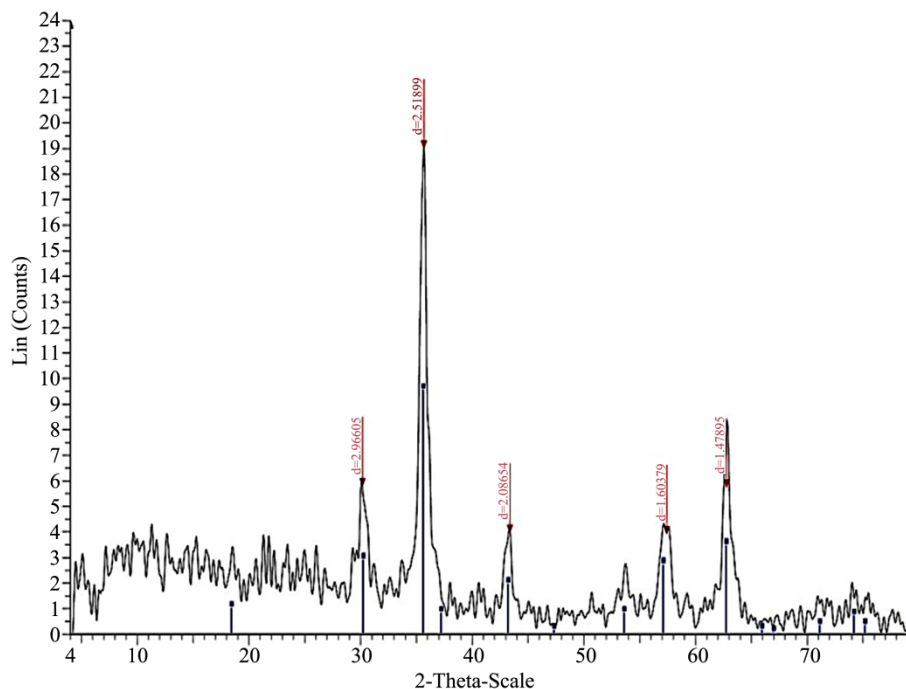


Fig. 2 — X-ray diffraction of Fe<sub>3</sub>O<sub>4</sub>-MNPs.

**Characterization of magnetic nano-adsorbents (FT-IR spectra, scan electron microscopy and transmission electron microscopy)**

The various functional groups immobilized on the  $\text{Fe}_3\text{O}_4$ -MNPs with or without using TEOS reagent were identified using Fourier transform-infrared absorption spectrometry (FT-IR). The resulting spectra are shown in Fig. 3. For the sample of pure magnetite, the vibrational bands at around  $584\text{ cm}^{-1}$  and  $631\text{ cm}^{-1}$  are characteristic of the (Fe–O) lattice vibrations<sup>29</sup> (Fig. 3a). In the case of using TEOS, the silica coated magnetite sample shows a band at  $1157\text{ cm}^{-1}$  and weak bands at  $1027$  and  $633\text{--}589\text{ cm}^{-1}$  corresponding to the stretching vibrations of (Si–Si), (Si–OH) and (Si–O–Fe), respectively<sup>30–32</sup>. These

bands are in good agreement with coating of  $\text{Fe}_3\text{O}_4$ -MNPs using tetraethylorthosilicate (TEOS) via conventional heating under reflux conditions<sup>26</sup>. The spectra of the products resulting from silylation using aminopropyltrimethoxysilane (APTMS) and chloropropyltrimethoxysilane (CPTMS) in presence and absence of TEOS were very similar. In the spectra of APTMS coated  $\text{Fe}_3\text{O}_4$ -MNPs- $\text{SiO}_2$  and  $\text{Fe}_3\text{O}_4$ -MNPs, the characteristic peak of the primary amine ( $-\text{NH}_2$ ) group was observed at  $3363\text{ cm}^{-1}$  and  $3361\text{ cm}^{-1}$ , respectively (Fig. 3b and 3c). However, in the spectra of 1,2-ethylenediamine (1,2-EDA) modified  $\text{Fe}_3\text{O}_4$ -MNPs- $\text{SiO}_2$ -CPTMS and  $\text{Fe}_3\text{O}_4$ -MNPs-CPTMS, the stretching band of (Si–OH)

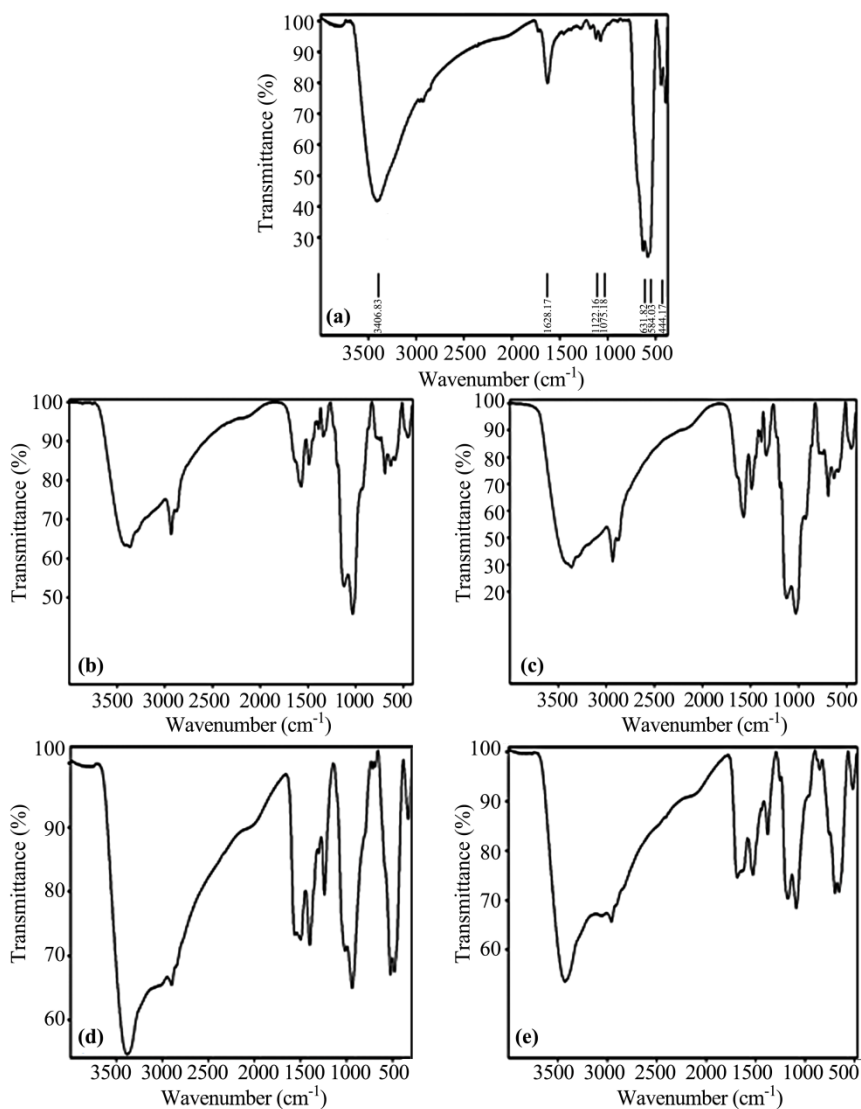


Fig. 3 — FT-IR spectra of (a)  $\text{Fe}_3\text{O}_4$ -MNPs, (b)  $\text{Fe}_3\text{O}_4$ -MNPs- $\text{SiO}_2$ -APTMS, (c)  $\text{Fe}_3\text{O}_4$ -MNPs-APTMS, (d)  $\text{Fe}_3\text{O}_4$ -MNPs- $\text{SiO}_2$ -CPTMS-1,2EDA and (e)  $\text{Fe}_3\text{O}_4$ -MNPs-CPTMS-1,2EDA.

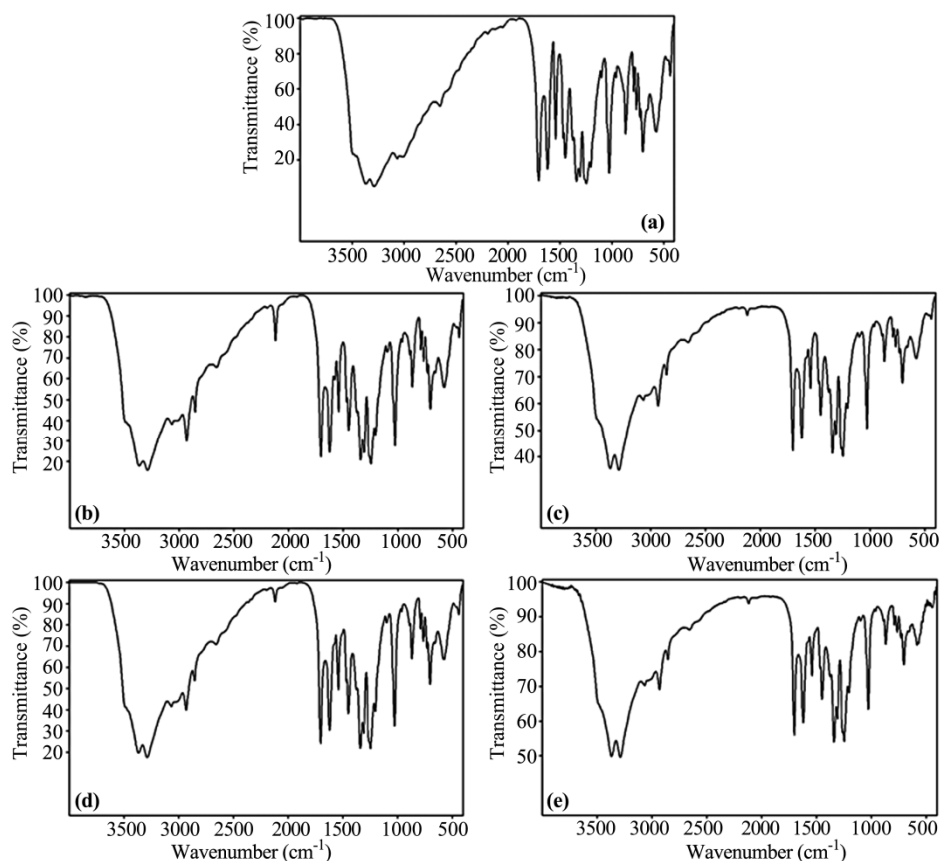


Fig. 4 — FT-IR spectra of (a) gallic acid (GA), (b)  $\text{Fe}_3\text{O}_4$ -MNPs-SiO<sub>2</sub>-APTMS-GA; (c)  $\text{Fe}_3\text{O}_4$ -MNPs-APTMS-GA; (d)  $\text{Fe}_3\text{O}_4$ -MNPs-SiO<sub>2</sub>-CPTMS-1,2EDA-GA and (e)  $\text{Fe}_3\text{O}_4$ -MNPs-CPTMS-1,2EDA-GA.

overlaps with the band of the (N-H) bending vibration at 3398 and 3416  $\text{cm}^{-1}$ , respectively<sup>32-34</sup>. In addition, a very weak band located at 1636 and 1637  $\text{cm}^{-1}$  in presence and absence of TEOS, respectively was argued to (C-N) stretching mode, Fig. 3d and 3e. Finally, the FT-IR spectra of the four amine functionalized magnetic nano-adsorbents ( $\text{Fe}_3\text{O}_4$ -MNPs-SiO<sub>2</sub>-APTMS,  $\text{Fe}_3\text{O}_4$ -MNPs-SiO<sub>2</sub>-CPTMS-1,2-EDA,  $\text{Fe}_3\text{O}_4$ -MNPs-APTMS and  $\text{Fe}_3\text{O}_4$ -MNPs-CPTMS-1,2-EDA) after grafting of gallic acid (GA) showed new bands at 1620-1624  $\text{cm}^{-1}$  and 1540  $\text{cm}^{-1}$ , characteristic for imide (-NHCO-) linkage<sup>34,35</sup> (Fig. 4 a-e). Moreover, the overall spectral changes were accompanied by drastic color change. Thus after gallic acid binding, the color changes from black or deep brown to dark yellow color (Fig. 1).

The morphological characteristics of the magnetic nanoparticles adsorbents ( $\text{Fe}_3\text{O}_4$ -MNPs-SiO<sub>2</sub>-APTMS,  $\text{Fe}_3\text{O}_4$ -MNPs-APTMS,  $\text{Fe}_3\text{O}_4$ -MNPs-SiO<sub>2</sub>-APTMS-GA and  $\text{Fe}_3\text{O}_4$ -MNPs-APTMS-GA) were investigated using SEM (Fig. 5). All SEM-images show homogeneous distribution of the particles. The image

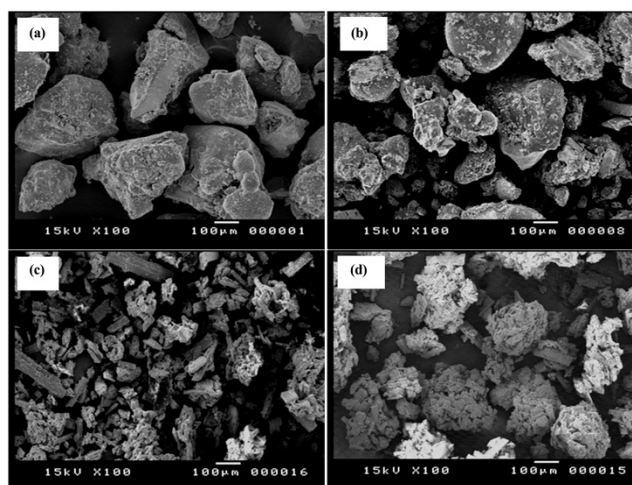


Fig. 5 — SEM of (a)  $\text{Fe}_3\text{O}_4$ -MNPs-SiO<sub>2</sub>-APTMS, (b)  $\text{Fe}_3\text{O}_4$ -MNPs-APTMS, (c)  $\text{Fe}_3\text{O}_4$ -MNPs-SiO<sub>2</sub>-APTMS-GA and (d)  $\text{Fe}_3\text{O}_4$ -MNPs-APTMS-GA.

shape and color of  $\text{Fe}_3\text{O}_4$ -MNPs-SiO<sub>2</sub>-APTMS,  $\text{Fe}_3\text{O}_4$ -MNPs-APTMS are almost similar as shown in Fig. 5a and 5b). Moreover, these magnetic nano-adsorbents are rough and porous, which could offer

high surface area<sup>36</sup>. However, the morphology of their surfaces after modification with gallic acid are quite different (rough with small particles), Fig. 5c and 5d which indicating successful loading of the modifiers on the amine magnetic nano-adsorbents surfaces<sup>37</sup>.

On the other hand, transmission electron microscopy (TEM) for synthesized adsorbents as shown in Fig. 6 illustrates the spherical shape of the particles along with their radius in nm. It was observed that adsorbents incorporated TEOS shell have particle size greater than their analogous without TEOS<sup>5,38</sup>. Particles size appeared in the range 9.55–13.8 nm for Fe<sub>3</sub>O<sub>4</sub>-MNPs-SiO<sub>2</sub>-APTMS and 8.65–11.6 nm for Fe<sub>3</sub>O<sub>4</sub>-MNPs-APTMS as shown in Fig. 6a and 6b. Also, they appeared in the range 13.3–15.5 nm for Fe<sub>3</sub>O<sub>4</sub>-MNPs-SiO<sub>2</sub>-APTMS-GA and 11.4–15.0 nm for Fe<sub>3</sub>O<sub>4</sub>-MNPs-APTMS-GA as shown in Fig 6c and 6d. In all cases, Fe<sub>3</sub>O<sub>4</sub>-MNPs after subsequent coating, amine functionalization and gallic acid grafting still maintained

their nano size. This means that the advantages of MNPs are also kept<sup>10</sup>.

#### Medium effect on the stability of the magnetic nano-adsorbents

Comparing the results of medium effects for the nano-adsorbents under investigation, synthesized in presence and in absence of TEOS, revealed that the two adsorbents Fe<sub>3</sub>O<sub>4</sub>-MNPs-SiO<sub>2</sub>-APTMS and Fe<sub>3</sub>O<sub>4</sub>-MNPs-APTMS behave in a similar manner regarding their stability, judging from their Cu(II) uptake capacity values in the pH range 3.0–10.0. The same trend was exhibited by the other two adsorbents Fe<sub>3</sub>O<sub>4</sub>-MNPs-SiO<sub>2</sub>-CPTMS-1,2-EDA and Fe<sub>3</sub>O<sub>4</sub>-MNPs-CPTMS-1,2-EDA where they gave the same Cu(II) uptake values in the pH range 5.0–10.0. Below pH 3.0 in the previous case and pH 5.0 in the latter case, adsorbents in which Fe<sub>3</sub>O<sub>4</sub>-MNPs directly coated with alkoxy silane were slightly more stable. These results as indicated graphically in Fig. 7

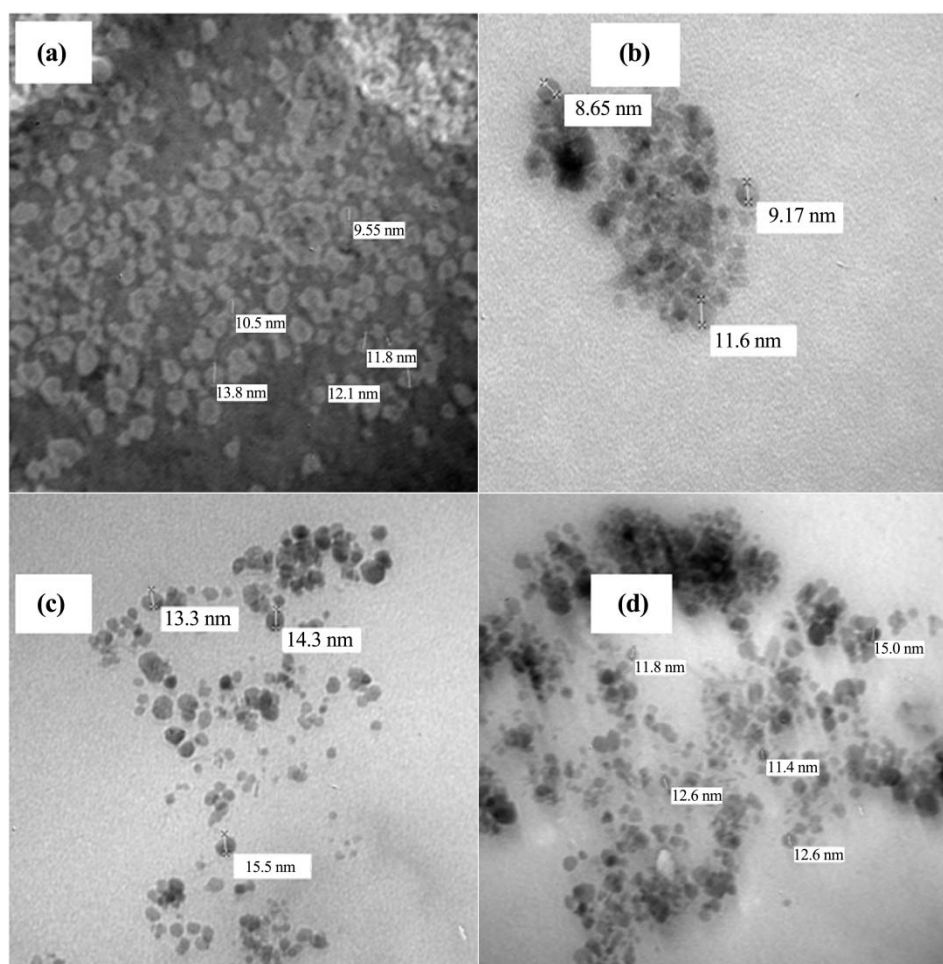


Fig. 6 — TEM of (a) Fe<sub>3</sub>O<sub>4</sub>-MNPs-SiO<sub>2</sub>-APTMS, (b) Fe<sub>3</sub>O<sub>4</sub>-MNPs-APTMS, (c) Fe<sub>3</sub>O<sub>4</sub>-MNPs-SiO<sub>2</sub>-APTMS-GA and (d) Fe<sub>3</sub>O<sub>4</sub>-MNPs-APTMS-GA.

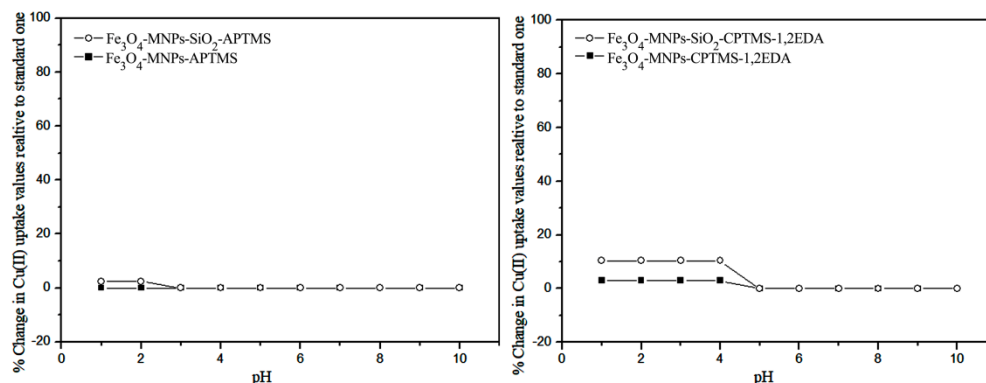


Fig. 7 — Effect of medium on the stability of magnetic nano-adsorbents.

support the bifunctional nature of alkoxy silanes for potential coating and amine functionalization.

#### Efficiency of Fe(III) uptake by gallic acid anchoring magnetic nano-adsorbent

It is well demonstrated that aliphatic functionalized adsorbents have great tendency for binding to Cu(II) ions<sup>39</sup>. They are also widely used as precursors for immobilizing different organic complexing agents to alter their affinity and maximize their analytical, environmental<sup>35,40,41</sup>, and catalytic<sup>42</sup> applications. So, it is important to explore the efficiency of the synthesized magnetic nano-adsorbents anchoring gallic acid (selective for Fe(III) binding<sup>43</sup>) for Fe(III) uptake. This was performed to validate the continuity of success of the direct protection mode of Fe<sub>3</sub>O<sub>4</sub>-MNPs adsorbent core via alkoxy silane interaction in comparison to conventional silica coating (Fe<sub>3</sub>O<sub>4</sub>-MNPs-SiO<sub>2</sub>) using TEOS. The results as shown in Fig. 8 and Table 1 illustrate great similarity between Fe(III) uptake-pH relationship profile along with too close uptake capacities, all at optimum pH 4.0 and under the same experimental batch conditions<sup>23,26</sup>. However, both the adsorbents Fe<sub>3</sub>O<sub>4</sub>-MNPs-SiO<sub>2</sub>-CPTMS-1,2-EDA-GA and MNPs-CPTMS-1,2-EDA-GA exhibit higher Fe(III) capacities (4.980 and 4.700 mmol/g) than their analogous Fe<sub>3</sub>O<sub>4</sub>-MNPs-SiO<sub>2</sub>-APTMS-GA and Fe<sub>3</sub>O<sub>4</sub>-MNPs-APTMS-GA (4.324 and 4.230 mmol/g) due to additional binding sites incorporated 1,2-ethylenediamine (1,2-EDA) moiety.

To support these results, other parameters such as the effect of adsorbent dosage and contact time were investigated, the results showed in Figs 9 and 10.

#### Adsorption studies

##### Adsorption kinetics

The kinetics of the adsorption process was investigated to study the effect of adsorption time of

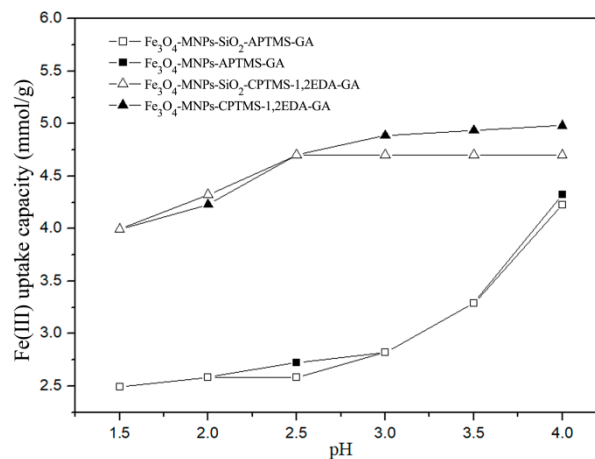


Fig. 8 — Effect of pH onto Fe(III) uptake values using magnetic nano-adsorbents.

Table 1 — Comparison of maximum Fe(III) uptake values (mmol/g) by the magnetic nano-adsorbents synthesized in presence and absence of TEOS

Magnetic nano-adsorbents	Maximum Fe(III) uptake values (mmol/g)*
Fe <sub>3</sub> O <sub>4</sub> -MNPs-SiO <sub>2</sub> -APTMS-GA	4.324
Fe <sub>3</sub> O <sub>4</sub> -MNPs-APTMS-GA	4.230
Fe <sub>3</sub> O <sub>4</sub> -MNPs-SiO <sub>2</sub> -CPTMS-1,2-EDA-GA	4.980
Fe <sub>3</sub> O <sub>4</sub> -MNPs-CPTMS-1,2-EDA-GA	4.700

\*Average mean of three replicate determinations (RSD = 0.1-0.5).

Fe(III) on the  $q_e$  value and the time required to achieve equilibrium between aqueous and solid phases. Two simple kinetic models, namely the pseudo-first-order and the pseudo-second-order, were the most often used to analyze the rate of adsorption. It was found that, Fe(III) was fast extracted on magnetic nano-adsorbents and the values of extraction remained constant with changing time. So, the adsorption kinetic data of Fe(III) was analyzed in



terms of pseudo-second-order sorption rather than pseudo-first-order. The pseudo-second-order equation is shown below<sup>44</sup>:

$$\frac{t}{q_t} = \frac{1}{v_o} + \frac{1}{q_t} t \quad \dots (1)$$

where,  $v_o = k_2 q_e^2$  is the initial adsorption rate ( $\text{mmol g}^{-1} \text{min}^{-1}$ ),  $k_2$  ( $\text{g mmol}^{-1} \text{min}^{-1}$ ) is the rate constant of adsorption,  $q_e$  and  $q_t$  ( $\text{mmol/g}$ ) is the

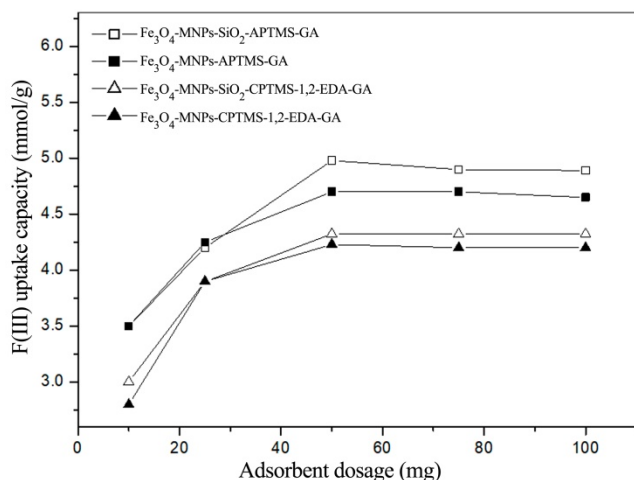


Fig. 9 — Effect of time onto Fe(III) uptake values using magnetic nano-adsorbents.

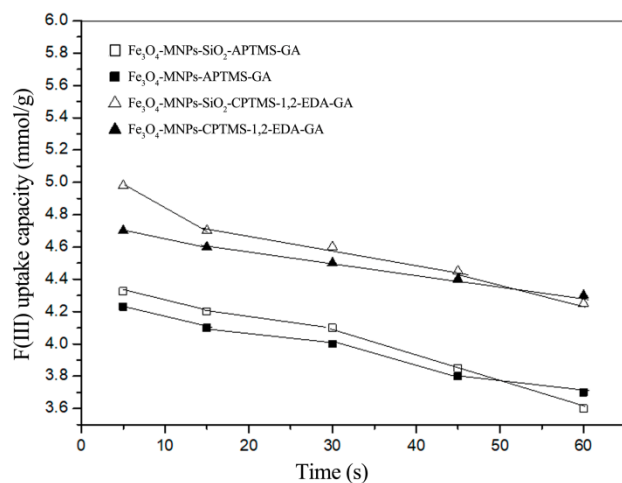


Fig. 10 — Effect of adsorbent dosage onto Fe(III) uptake values using magnetic nano-adsorbents.

amount of metal ion sorbet on adsorbent surface at equilibrium and time  $t$  (min), respectively.  $v_o$  and  $q_e$  can be obtained from the intercept and slope of a plot of  $t/q_t$  versus  $t$  (Fig. 11). The experimental values of  $v_o$ ,  $q_e$  and  $k_2$  values were showed in Table 2. The calculated  $q_e$  values for the four adsorbents were agreed very well with the experimental values  $q_t$  with high values of  $R^2$ . This explained that the model can be applied for the entire adsorption process and confirms the adsorption of Fe(III) onto the nano-adsorbents.

### Adsorption isotherms

Adsorption isotherms were studied to explore the adsorption mechanism of Fe(III) on the adsorbents. Two adsorption isotherm equations were used to fit the experimental data, which were Langmuir and Freundlich equations<sup>44</sup>. Langmuir model tends to describe monolayer adsorption which assumes that the adsorbent surface is uniform, adsorption energy is the same everywhere and each active center can adsorb only one molecule. Freundlich model is usually applied to multi-molecular adsorption on uneven surface, especially physical adsorption and chemical adsorption. The two adsorption isotherm equations are expressed as Eqns 2 and 3, respectively.

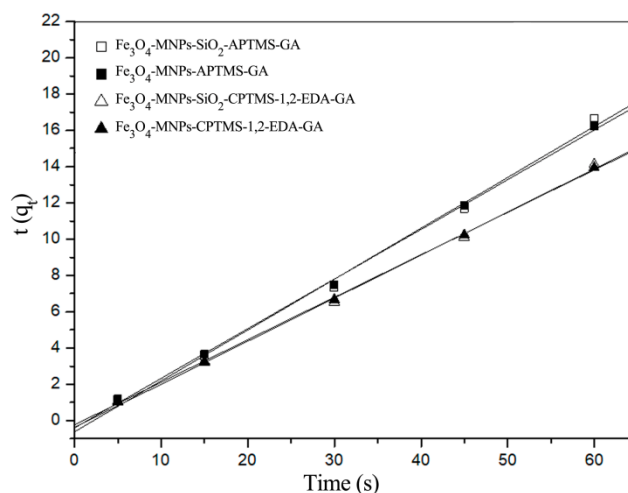


Fig. 11 — Pseudo-second-order kinetic model of Fe(III) using magnetic nano-adsorbents.

Table 2 — Adsorption kinetic parameters modeled by pseudo second-order equation for adsorption of Fe(III) by the magnetic nano-adsorbents synthesized in presence and absence of TEOS

Adsorbent	$q_e$ (mmol/g)	$q_t$ (mmol/g)	$v_o$ ( $\text{mmol g}^{-1} \text{min}^{-1}$ )	$k_2$ ( $\text{g mmol}^{-1} \text{min}^{-1}$ )	$R^2$
$\text{Fe}_3\text{O}_4\text{-MNPs-SiO}_2\text{-APTMS-GA}$	4.324	4.273	1.634	0.0874	0.99872
$\text{Fe}_3\text{O}_4\text{-MNPs-APTMS-GA}$	4.230	4.155	2.45	0.1369	0.99936
$\text{Fe}_3\text{O}_4\text{-MNPs-SiO}_2\text{-CPTMS-1,2-EDA-GA}$	4.980	4.851	2.72	0.1097	0.99915
$\text{Fe}_3\text{O}_4\text{-MNPs-CPTMS-1,2-EDA-GA}$	4.700	4.576	4.47	0.2023	0.99975

$q_e$  and  $q_t$  ( $\text{mmol/g}$ ) is the amount of metal ion sorbet on adsorbent surface at equilibrium and any time  $t$ .

$$\text{Langmuir isotherm: } \frac{1}{q_e} = \frac{1}{q_{\max}} + \frac{1}{q_{\max}} K_L C_e \quad \dots (2)$$

(linear form)

$$\text{Freundlich isotherm: } \log q_e = \log K_f + \frac{1}{n} \log C_e \quad \dots (3)$$

(linear form)

where  $q_e$  (mmol/g) is adsorption capacity at equilibrium,  $q_{\max}$  (mmol/g) is saturated adsorption capacity,  $C_e$  ( $\text{m L}^{-1}$ ) is Fe(III) concentration at equilibrium,  $K_L$  is adsorption equilibrium constant of Langmuir adsorption isotherm (indicates the nature of sorption and the shape of the isotherm accordingly),  $K_f$  and  $n$  are Freundlich constants related to adsorption capacity and adsorption strength. Moreover, the essential characteristics of the Langmuir isotherm can also be expressed in terms of a dimensionless constant separation factor or equilibrium parameter,  $R_L$ , which is defined as  $R_L = 1/(1 + K_L C_0)$ , where  $C_0$  the initial concentration of the analyte. The  $R_L$  value indicates the type of the isotherm. The adsorption isotherm results for all adsorbents are listed in Table 3. According to the results, the values of  $1/n$  for Freundlich model were lower than one and  $R_L$  values for Langmuir model were between 0–1, which show favorable sorption of Fe(III) by the four adsorbents<sup>45</sup>.

## Application

### Adsorbent regeneration studies

The application of the four adsorbents for further extraction of Fe(III) after first use requires an efficient method for their reuse. In fact, regeneration using acid or base treatment as in ion-exchangers is not adequate for the nano-adsorbents, because acid or base treatment may increase the chance of hydrolysis of the bound complexing agent. Therefore, it was selected to use another strong complexing agent such as ethylenediaminetetraacetic acid (EDTA) to back-extract the metal ion from metal chelate formed modified adsorbent in the regeneration process. Thus Fe(III)-adsorbent complexes were mixed with excess (0.1 M-EDTA) solution and shaken for 60 min,

filtered off, washed with double distilled water and dried. 300.0 mg of each treated adsorbent, along with untreated one taken as standard were used to evaluate the metal ion percentage extraction for Fe(III), under the same batch conditions which described previously at the optimum pH value. The percentage extraction determined after the second extraction were very close to percentage extraction found in the first one with percentage decrease in efficiency not exceeding 1.2% for both adsorbents. The efficiency of adsorbent regeneration was obtained using the following equation:

$$E. R. = \frac{\text{total adsorption capacity in the second run}}{\text{total adsorption capacity in the first run}} \times 100 \quad \dots (4)$$

It can be seen that the removal efficiency values of Fe(III) using Fe<sub>3</sub>O<sub>4</sub>-MNPs-SiO<sub>2</sub>-APTMS, Fe<sub>3</sub>O<sub>4</sub>-MNPs-APTMS, Fe<sub>3</sub>O<sub>4</sub>-MNPs-SiO<sub>2</sub>-APTMS-GA and Fe<sub>3</sub>O<sub>4</sub>-MNPs-APTMS-GA were  $98.89 \pm 0.1$ ,  $98.97 \pm 0.2$ ,  $99.97 \pm 0.05$  and  $99.99 \pm 0.1\%$ , respectively after cycle 3 times, which remained the removal efficiency compared to 99.98% at first time, indicating that the adsorbents can be recycled for the removal of Fe(III) in water treatment.

### Extraction of trace concentrations of Fe(III) spiked natural water samples

Uptake experiments were carried out under batch conditions using different natural water samples: ground water (GW), natural drinking water (NDW), sea water (SW) and tap water (TW). A 150.0 mg of adsorbent was conditioned with 50.0 mL of water sample spiked Fe(III) at concentration of 5.0 ppm (adjusted at pH 4.0 by fine addition of concentrated HCl) with shaking for 5 s<sup>23,26</sup>. 10.0 mL of the solution (free from the suspended adsorbent) were taken at the end of the experiment where the residual concentration of metal ion was determined via FAAS. The percentage recovery values of Fe(III) were combined in Table 4. The results support the equal capability of the nano-adsorbents for removal of Fe(III) with the same efficiency.

Table 3 — Adsorption isotherm parameters modeled by Langmuir and Freundlich

Adsorbent	Langmuir constants			Freundlich constants		
	$R_L$	$q_{\max}^a$	$R^2$	$K_f$	$1/n$	$R^2$
Fe <sub>3</sub> O <sub>4</sub> -MNPs-SiO <sub>2</sub> -APTMS-GA	0.23	4.282	0.99985	4.603	0.711	0.9159
Fe <sub>3</sub> O <sub>4</sub> -MNPs-APTMS-GA	0.21	4.863	0.99892	4.879	0.678	0.92092
Fe <sub>3</sub> O <sub>4</sub> -MNPs-SiO <sub>2</sub> -CPTMS-1,2-EDA-GA	0.34	4.840	0.99896	5.998	0.565	0.90051
Fe <sub>3</sub> O <sub>4</sub> -MNPs-CPTMS-1,2-EDA-GA	0.41	4.598	0.99974	5.789	0.523	0.89577

<sup>a</sup> mmol/gm

Table 4 — Comparison of percentage recovery of Fe(III) spiked different natural water samples

Magnetic nano-adsorbents	%Recovery*			
	GW	NDW	SW	TW
Fe <sub>3</sub> O <sub>4</sub> -MNPs-SiO <sub>2</sub> -APTMS-GA	96.94%	92.78%	93.92%	94.26%
Fe <sub>3</sub> O <sub>4</sub> -MNPs-APTMS-GA	95.00%	92.87%	91.18%	94.70%
Fe <sub>3</sub> O <sub>4</sub> -MNPs-SiO <sub>2</sub> -CPTMS-1,2-EDA-GA	93.95%	92.94%	90.60%	91.68%
Fe <sub>3</sub> O <sub>4</sub> -MNPs-CPTMS-1,2-EDA-GA	93.14%	92.08%	90.42%	93.00%

\*Average mean of three replicate determinations (RSD = 0.5-1.0)

GW= ground water, NDW= natural drinking water, SW= sea water, TW= tap water

Table 5 — Comparison of present method with other reported literature for Fe(III)

Adsorbent	pH	Shaking time	Metal capacity ( $\mu\text{mol g}^{-1}$ )	Ref.
sugar cane bagasse	2	60 min	100	46
Hybrid inorganic/organic alumina adsorbents-functionalized-purpurogallin	4	5 min	560	47
Alumina modified with phenolic compounds	3.5	15–30 min	1100	48
gallic acid anchored iron magnetic nano-adsorbents	4	5 s	(4230 to 4980)	This work

### Comparison with other methods

The present developed method was compared with those reported in literature. The obtained results indicated that our adsorbents have higher efficiency for Fe(III) than the other adsorbents as given in Table 5. Furthermore, the direct and fast separation of Fe(III) due to the use of magnetic nano-adsorbents is significant.

### Conclusions

For amine functionalization of Fe<sub>3</sub>O<sub>4</sub>-MNPs they were first protected to prevent tendency for aggregation in aqueous medium and to enhance chemical stability against medium effects. Two routes were followed to achieve potential coating process. In the first, a conventional coating utilizing TEOS is performed yielding silica coated MNPs (Fe<sub>3</sub>O<sub>4</sub>-MNPs-SiO<sub>2</sub>). It is further amine functionalized either by direct interaction with aminopropyltrimethoxysilane (APTMS) to give Fe<sub>3</sub>O<sub>4</sub>-MNPs-SiO<sub>2</sub>-APTMS or indirect using chloropropyltrimethoxysilane, followed by interaction with 1,2-ethylenediamine (1,2-EDA) to give the adsorbent Fe<sub>3</sub>O<sub>4</sub>-MNPs-SiO<sub>2</sub>-CPTMS-1,2-EDA which is further functionalized by anchoring gallic acid to give the adsorbent Fe<sub>3</sub>O<sub>4</sub>-MNPs-SiO<sub>2</sub>-CPTMS-1,2-EDA-GA. In the second, the bifunctional character of the alkoxy silane (APTMS) is adapted. Thus, a coated and amine functionalized adsorbent (Fe<sub>3</sub>O<sub>4</sub>-MNPs-APTMS) could be produced directly and in a single step. On the other hand, indirect amine functionalization using CPTMS followed by 1,2-EDA produced the adsorbent Fe<sub>3</sub>O<sub>4</sub>-MNPs-CPTMS-1,2-

EDA. Finally, gallic acid functionalization produced the adsorbent Fe<sub>3</sub>O<sub>4</sub>-MNPs-CPTMS-1,2-EDA-GA.

Comparing characteristic FT-IR spectral bands, SEM and TEM images for the adsorbents produced in both cases (in presence and absence of TEOS) proved very similar appearance, denoting successful coating, amine functionalization and GA grafting. This reflected in similar trend with respect to medium stability, judging from values of Cu(II) uptake exhibited by amine functionalized adsorbents in the range of pH studied. This is in addition to, identical or non-significant differences either for uptake of Fe(III) values or percentage extraction of trace Fe(III) concentration spiked natural water samples. In short, application of established microwave-solvent free irradiation technique for all over modification process of Fe<sub>3</sub>O<sub>4</sub> core based adsorbent, side by side to direct silylation using alkoxy silanes (APTMS and CPTMS) reduce a step in modification Scheme accompanied by drastic reduction in time required for coating, amine functionalization and grafting of the selected organic moiety.

### References

- 1 Turiel E, Martin-Esteban A & Tadeo J L, *J Chromatogr A*, 1172 (2007) 97.
- 2 Kim J, Kim H S, Lee N, Kim T, Kim H, Yu T, Song I C, Moon W K & Hyeon T, *Angew Chem Int Ed Eng*, 47 (2008) 8438.
- 3 Nomura A, Shin S, Mehdi O O & Kauffmann J M, *Anal Chem*, 76 (2004) 5498.
- 4 Bilkova' Z, Slova'kova' M, Lyka A, Hora'k D, Lenfeld J, Turkova' J & Chura'ek J, *J Chromatogr, B* 770 (2002) 25.
- 5 Chen L, Wang T & Tong J, *Trends in Anal Chem* 30 (2011) 1095.
- 6 Wang Y, Luo X, Tang J, Hu X, Xu Q & Yang C, *Anal Chim Acta*, 713 (2012) 92.

- 7 Mei J, Zhang L & Niu Y, *Mater Res Bull*, 70 (2015) 82.
- 8 Dutta A K, Maji S K & Adhikary B, *Mater Res Bull*, 49 (2014) 28.
- 9 Wang L, Tian C, Mu G, Sun L, Zhang H & Fu H, *Mater Res Bull*, 47 (2012) 646.
- 10 Chen L & Li B, *Anal Methods*, 4 (2012) 2613.
- 11 Jiang H M, Yan Z P, Zhao Y, Hu X & Lian H Z, *Talanta*, 94 (2012) 251.
- 12 Cui H, Li D & Zhang Z, *Materials Lett*, 143 (2015) 38.
- 13 Faraji M, Yamini Y, Saleh A, Rezaee M, Ghambarian M & Hassani R, *Anal Chim Acta*, 659 (2010) 172.
- 14 Huang Y F, Jiang Y & Yan X P, *J Anal At Spectrom*, 25 (2010) 1467.
- 15 Yamauraa M, Camiloa R L, Sampaio L C, Macedoc M A, Nakamurad M & Tomad H E, *J Mag Mag Mater*, 279 (2004) 210.
- 16 Giakisikli G & Anthemidis A N, *Anal Chim Acta*, 789 (2013) 1.
- 17 Demin A M, Krasnov V P & Charushin V N, *Mendeleev Comm*, 23 (2013) 14.
- 18 A del Campoa A, Sena T, Lellouchec J P & Bruce I J, *J Mag Mag Mater*, 293 (2005) 33.
- 19 Mamdouh S M, Alaa E A, Sawsan S H & Nessma M N, *Spectrochimica Acta Part A: Molecular and Biomolecular Spectroscopy*, 120 (2014) 505.
- 20 Bahadur N M, Furusawa T, Sato M, Kurayama F, Siddiquey I A & Suzuki N, *J Colloid Inter Sci*, 355 (2011) 312.
- 21 Varma R S, *Green Chem*, 1 (1999) 43.
- 22 Lidstrom P, Tierney J, Wathey B & Westman J, *Tetrahedron*, 57 (2001) 9225.
- 23 Ahmed S A & Soliman E M, *Anal Sci*, 31 (2015) 1047.
- 24 Soliman E M, Marwani H M & Albishri H M, *Environ Monit Assess*, 185 (2013) 10269.
- 25 Ahmed S A, *J Hazard Mater*, 156 (2008) 521.
- 26 Ahmed S A & Soliman E M, *Anal Sci*, 30 (2014) 823.
- 27 Arabi H, Nateghi S & Sadeghi S, *Solid State Phenom*, 152–153 (2009) 205.
- 28 Klug H P & Alexander L E, *X-ray Diffraction Procedures for Polycrystalline and Amorphous Materials*, (John Wiley and Sons, New York) 1962.
- 29 Cornell R M & Schwertmann U, *The iron oxides*, (Second ed, Wiley-VCH) 2003.
- 30 Mahmoud M E, El-Essawi M M & Fathallah E M I, *J Liq Chromatogr Relat Technol*, 27 (2004) 1711.
- 31 Goubert-Renaudin S, Schneider R & Walcarius A, *Tetrahedron Lett*, 48 (2007) 2113.
- 32 Bruce I J & Sen T, *Langmuir*, 21 (2005) 7029.
- 33 Venkatesan K A, Srinasan T G & Rao P R V, *Colloids Surf A*, 180 (2001) 277.
- 34 Girginova P I, Daniel-da-Silva A L, Lopes C B, Figueira P, Otero M, Amaral V S, Pereira E & Trindade T, *J Colloid Inter Sci*, 345 (2010) 234.
- 35 Jang J H & Lim H B, *Microchem J*, 94 (2010) 148.
- 36 Zhang N, Peng H & Hu B, *Talanta*, 94 (2012) 278.
- 37 Anirudhan T S, Divya P L & Nima, *J Mater Sci Eng C*, 55 (2015) 471.
- 38 Siddiquey I A, Furusawa T, Hoshi Y, Ukaji E, Kurayama F, Sato M & Suzuki N, *App Surf Sci*, 255 (2008) 2419.
- 39 Chethan P D & Vishalakshi B, *Carbohydrate Polym*, 97 (2013) 530.
- 40 Sadeghi S, Azhdari H, Arabi H & Moghaddam A Z, *J Hazard Mater*, 215–216 (2012) 208.
- 41 Wierucka M & Biziuk M, *Trends in Anal Chem*, 59 (2014) 50.
- 42 Wang H B, Zhang Y H, Zhang Y B, Zhang F W, Niu J R, Yang H L, Li R & Maa J T, *Solid State Sci*, 14 (2012) 1256.
- 43 Fazary A E, Taha M & Ju Y H, *J Chem Eng Data*, 54 (2009) 32.
- 44 Salwa A A, Ahmed A A & Asmaa M A, *Appl Water Sci*, 7 (2017) 677.
- 45 Mohammad A F & Brian B *J Mol Liq*, 249 (2018) 193.
- 46 Ezzat M S, Salwa A A & Aliaa A F, *Arabian J Chem*, 4 (2011) 63.
- 47 Mohamed E M, Osama F H, Maher M O, Amr A Y & Ahmed A, *J Hazard Mater* 176 (2010) 906.
- 48 Salwa A A, *Ind J Chem*, 54A (2015) 324.